Planta (2010) 232:887–898
DOI 10.1007/s00425-010-1227-5

ORIGINAL ARTICLE

Acclimation of photosynthesis to nitrogen deficiency in *Phaseolus vulgaris*

Taras Antal · Heta Mattila · Marja Hakala-Yatkin · Taina Tyystjärvi · Esa Tyystjärvi

Received: 25 March 2010 / Accepted: 6 July 2010 / Published online: 15 July 2010

Abstract Nitrogen deficiency diminishes consumption of photosynthates in anabolic metabolism. We studied adjustments of the photosynthetic machinery in nitrogen-deficient bean plants and found four phenomena. First, the number of chloroplasts per cell decreased. Chloroplasts of nitrogen starved leaves contained less pigments than those of control leaves, but the in vitro activities of light reactions did not change when measured on chlorophyll basis. Second, nitrogen deficiency induced cyclic electron transfer. The amounts of Rubisco and ferredoxin-NADP$^+$ reductase decreased in nitrogen starved plants. Low activities of these enzymes are expected to lead to increase in reduction of oxygen by photosystem I. However, diaminobenzidine staining did not reveal hydrogen peroxide production in nitrogen starved plants. Measurements of far-red-light-induced redox changes of the primary donor of photosystem I suggested that instead of producing oxygen radicals, nitrogen starved plants develop a high activity of cyclic electron transport that competes with oxygen for electrons. Nitrogen starvation led to decrease in photochemical quenching and increase in non-photochemical quenching, indicating that cyclic electron transport reduces the plastoquinone pool and acidifies the lumen. A third effect is redistribution of excitation energy between the photosystems in favor of photosystem I. Thus, thylakoids of nitrogen starved plants appeared to be locked in state 2, which further protects photosystem II by decreasing its absorption cross-section. As a fourth response, the proportion of non-Q_B-reducing photosystem II reaction centers increased and the redox potential of the Q_B/Q_B^- pair decreased by 25 mV in a fraction of photosystem II centers of nitrogen starved plants.

Keywords Nitrogen deficiency · *Phaseolus* · Photosynthesis · Regulation

Abbreviations

N	Nitrogen
LN	Low nitrogen
HN	High nitrogen
Chl	Chlorophyll
PQ	Plastoquinone
Rubisco	Ribulose-1,5-bisphosphate carboxylase/oxygenase
FNR	Ferredoxin-NADP$^+$ reductase
OEC	Oxygen evolving complex
CET	Cyclic electron flow around photosystem I
PPFD	Photosynthetic photon flux density
TL	Thermoluminescence
DCMU	3-(3,4-Dichlorophenyl)-1,1-dimethylurea
DCBQ	2,6-Dichlorobenzoquinone
DCIP	Dichlorophenol-indophenol
DAB	3,3-Diaminobenzidine

Introduction

Nitrogen (N) is a mineral element that plants require in greatest amount and it is often the growth limiting nutrient. Chlorophyll (Chl) concentration, photosynthesis rate and growth have been observed to decrease with N deficiency (Evans and Terashima 1987; Marschner 1995). Both the

T. Antal · H. Mattila · M. Hakala-Yatkin · T. Tyystjärvi · E. Tyystjärvi (✉)
Molecular Plant Biology, Department of Biochemistry and Food Chemistry, University of Turku, 20014 Turku, Finland
e-mail: esatyy@utu.fi

light-saturated rate (Sage and Pearcy 1987; Terashima and Evans 1988) and the quantum yield of photosynthesis (Lawlor et al. 1987) are low in N starved plants. The rate of CO_2 assimilation per Chl unit declines due to decrease in the expression of several key enzymes of the Calvin–Benson cycle (Evans and Terashima 1987; Sage and Pearcy 1987; Terashima and Evans 1988; Sugiharto et al. 1990). Moreover, N deficiency induces accumulation of starch (Kutik et al. 1995; Bondada and Syvertsen 2003), apparently because N deficiency limits the consumption of carbohydrates in anabolic reactions.

While N deficiency decreases CO_2 fixation, photosynthetic electron transport usually remains active (Evans and Terashima 1987). The imbalance between production and consumption of ATP and NADPH may result in over-reduction of the photosynthetic electron transport chain in the light, potentially promoting harmful side reactions generating reactive oxygen species. Superoxide, O_2^-, is produced at the acceptor side of PS I (reviewed by Asada 2006), while over-reduction of electron carriers of PS II promote charge recombination reactions that have been suggested to lead to production of singlet oxygen (Keren et al. 1997).

Non-photochemical quenching of excitation energy in PS II and down-regulation of electron transport via the cytochrome b_6/f complex are feed-back mechanisms that adjust the rate of photosynthetic electron transport to match the rate of consumption of NAD(P)H and ATP. These mechanisms are activated under different stress conditions and their activities depend on the pH gradient across the thylakoid membrane (Pascal et al. 2005; Laisk et al. 2005). Furthermore, high NAD(P)H/NAD(P)$^+$ ratio may also down-regulate photosynthetic electron transport when the Calvin–Benson cycle runs slowly (Hald et al. 2008).

In this work, we have investigated how N deficiency affects the composition of thylakoids and activities of the light reactions in bean plants. Particular attention has been paid to the acceptor side of PS II. We have further examined the regulatory mechanisms allowing N starved plants to avoid oxidative stress and to prevent over-accumulation of reducing equivalents in chloroplasts. Switching from linear to cyclic electron flow, redistribution of excitation energy between PS II and PS I in favor of PS I, and down-regulation of chloroplast division are proposed to participate in acclimation to N deficiency.

Materials and methods

Plant material and growth conditions

Bean (*Phaseolus vulgaris* L. cv Saxa, obtained from Bröderna Nelsons Frö, Tingsryd, Sweden) seeds were sown in vermiculite. After 1 week, the plantlets were moved to a hydroponic nutrient medium (Hoagland and Arnon 1950). Control plants (designated as HN for high nitrogen) were grown in standard medium containing 12 mM NO_3^- and 1 mM NH_4^+ whereas the medium for low nitrogen (LN) plants contained only 1% of nitrate and ammonia of the standard medium. The solutions were buffered with 2 mM Mes-KOH, pH 5.5, and continuously aerated. Cl^- was used to compensate for NO_3^-, and concentrations of all other ions were within the range of 91–100% of the concentration of the control solution. Nine plants were placed in each container with 5 l of nutrient solution, and the solution was changed twice a week. The plants were grown at 22°C in a 16-h light/8-h dark rhythm for 10 days. The photosynthetic photon flux density (PPFD) of the growth light was 120–140 μmol m^{-2} s^{-1}. Nodule formation did not occur in the roots.

Confocal microscopy

Images were obtained with an inverted confocal laser scanning microscope (Zeiss LSM510 META; http://www.zeiss.com) with a 20×/0.50 water objective. Chloroplasts were imaged by Chl autofluorescence excited at 488 nm with an argon diode laser and detected through a 650 nm emission filter. Maximal projections of the sequential confocal images of the uppermost mesophyll cell layer were created with Zeiss LSM Image Browser.

Isolation of thylakoids and preparation of crude extracts

Thylakoids were isolated according to Hakala et al. (2005) and stored at −70°C until use. For measurements, thylakoids were thawed in the dark on ice. The excess of starch was removed by a series of short (4–6 s) centrifugations at 1500*g*. Thereafter, thylakoids were suspended either in PS II buffer (40 mM Hepes–KOH, pH 7.6; 0.33 M sorbitol, 5 mM $MgCl_2$, 5 mM NaCl, 1 M glycine betaine, 1 mM KH_2PO_4, and 5 mM NH_2Cl) or storage buffer (40 mM Hepes–KOH, pH 7.6; 0.33 M sorbitol, 5 mM $MgCl_2$, 5 mM NaCl) as indicated. Crude extracts were prepared by grinding the leaves on liquid nitrogen followed by suspension to storage buffer and filtration through Miracloth (Calbiochem, San Diego, USA).

O_2 evolution and electron transport measurements

Thylakoids were diluted to 10 μg Chl ml^{-1} in PS II buffer. The light-saturated rate of oxygen evolution was measured with a Hansatech (King's Lynn, UK) oxygen electrode by using 0.125 mM 2,6-dichlorobenzoquinone (DCBQ) as electron acceptor. The rate of electron flow from reduced dichlorophenol-indophenol (DCPIP•H_2) to methyl viologen (MV) was assayed as O_2 uptake (Curtis et al. 1975)

with a Hansatech oxygen electrode in saturating light. The light-saturated rate of reduction of 80 μM DCPIP was measured spectrophotometrically at 590 nm; the reaction rate was stable for approximately 5 min.

Determination of pigment and protein content

The xanthophyll composition of thylakoids was measured with high pressure liquid chromatography using Agilent 1100 chromatograph equipped with a reverse phase C8 column (Zorbax Eclipse XDB-C8, Agilent). The Chl content of thylakoids and crude extracts was determined according to Porra et al. (1989). The Chl concentrations of leaves were determined by using *N*,*N*-dimethylformamide as a solvent (Inskeep and Bloom 1985). Protein concentrations of HN and LN leaves were measured from leaf extract with the DC protein assay kit (Biorad, Hercules, CA, USA) using bovine serum albumin as a standard.

Chl fluorescence measurements

For measurements of Chl fluorescence quenching, leaves were dark adapted for 2 h. Fluorescence was measured with a PAM-101 fluorometer (Heinz Walz GmbH, Effeltrich, Germany). First, minimum fluorescence in dark adapted state (F_0) was measured with weak measuring light alone. A saturating light pulse (1 s, PPFD 5,000 μmol m^{-2} s^{-1}) was used to obtain maximum fluorescence (F_M). Actinic white light (PPFD 300 μmol m^{-2} s^{-1}) was then switched on for 20 min and the maximum fluorescence yield during continuous illumination (F_M') was measured with saturating flashes. To determine the minimum fluorescence yield in light adapted state (F_0') actinic light was switched off and the leaf was given 2 s of far-red light (>700 nm) to oxidize Q_A, followed by a series of 0.1-s pulses of measuring light with 0.5-s darkness between these pulses. F_0' was obtained by interpolating the fluorescence values to the time when the actinic light was switched off. The FIP fluorescence software (Tyystjärvi and Karunen 1990) was used to drive the fluorometer and to analyze the results. We used the parameter $\mathrm{NPQ} = \frac{F_M - F_M'}{F_M'}$ (Bilger and Björkman 1990) to measure non-photochemical quenching of excitation energy and $q_P = \frac{F_M' - F_S}{F_M' - F_0'}$ (Schreiber et al. 1986) to describe photochemical quenching. The fluorescence intensity under continuous illumination (F_S) was measured before the saturating pulse.

Flash-induced increase and the subsequent relaxation of fluorescence yield were measured with a double-modulation fluorometer (PSI, Brno, Czech Republic) as described in Allahverdiyeva et al. (2004). Thylakoids (10 μg Chl ml^{-1}) were suspended in PS II buffer.

77 K Chl fluorescence emission spectra of crude extracts were measured with a diode array fiber-optic spectrophotometer (USB4000, Ocean Optics, Eerbeek, The Netherlands). Samples were excited with a slide projector through a 500 nm short-pass Corion cutoff filter (Newport Corp., Franklin, MA, USA). The sample (20 μl, 10 μg Chl ml^{-1} in storage buffer) was placed in a microcentrifuge tube and frozen in liquid N_2 with a fiber-optic probe fixed close to the surface.

Rapid light response curves were measured with a PAM-2000 fluorometer (Walz). For each measurement, a leaf was dark incubated for 30 min and then brought under the probe of the fluorometer. The F_0 and F_M levels were first measured using the measuring beam alone and a saturating flash (0.8 s, PPFD 5,000 μmol m^{-2} s^{-1}), and then the leaf was illuminated with a series of PPFD values, starting from 10 μmol m^{-2} s^{-1}. Illumination at each PPFD value was continued for 2 min, and a saturating pulse was then fired to measure F_M'. ETR was calculated as $0.84 \times 0.5 \times (F_M' - F_S)/F_M'$, where F_S is the steady-state level of fluorescence measured before the flash. The results were fitted to the non-rectangular hyperbolic model of photosynthetic light response (Jassby and Platt 1976), omitting dark respiration.

Thermoluminescence

Thermoluminescence bands were recorded with a home-made luminometer as described earlier (Tyystjärvi et al. 2009). The bands were analyzed using the Eyring theory of reaction rates (Glasstone et al. 1941) and numerically fitted with the ModelMaker 4 software (ModelKinetics, Oxfordshire, UK).

P_{700} redox transitions

Spectroscopic measurements were performed on intact leaves with a Joliot type spectrometer (JTS-10; Bio-Logic SAS, Grenoble) as described in (Joliot and Joliot 2005). P_{700} redox transitions were assessed at 705 nm. Before measurement, the leaves were dark adapted for 2 h, then pre-illuminated for 20 s with far-red light to switch electron flow into the linear mode (Joliot and Joliot 2005), and finally kept in the dark for 20 s before the measurement. P_{700} oxidation was then induced by a strong pulse of far-red illumination (2,500 μmol m^{-2} s^{-1}) peaking at 720 nm and filtered through a 700 nm long-pass cutoff filter. After the FR-pulse, reduction of P_{700}^+ in the dark was also followed. A low signal associated with Chl fluorescence emission was subtracted from the kinetics.

Immunoblotting

Proteins from crude extracts and thylakoid samples were separated by using 10% NEXT GEL SDS–PAGE according to the manufacturer's instructions (Amresco Inc., Solon, OH, USA). Samples were solubilized for 5 min at 70°C using the NEXT GEL^{TM} sample solubilization buffer (Amresco). After electrophoresis, proteins were transferred to Immobilon-P membranes (Millipore Corp., Billerica, MA, USA). For D1 protein detection, thylakoid samples containing 2 μg Chl were loaded in each well, and a commercial D1 protein antibody (AS06 124A, Agrisera AB, Vännäs, Sweden) was used. For detection of Rubisco, crude extract samples containing 0.3 μg Chl were loaded in each well. The Rubisco antibody (AS01 017S, Agrisera) recognized the large subunit of Rubisco. For detection of ferredoxin-NADP$^+$ reductase (FNR) crude extract samples containing 1.5 μg Chl were loaded in each well. The FNR antibody was a generous gift from Dr. Paula Mulo. The Goat Anti-Rabbit IgG (H + L) alkaline phosphatase conjugate (Zymed, San Fransisco, CA, USA) and the CDP star chemiluminescence kit (New England Biolabs, Ipswich, MA, USA) were used for detection in western blotting.

DAB staining

The accumulation of H_2O_2 in leaves was studied with the 3,3-diaminobenzidine (DAB) method as described by Ren et al. (2002).

Results

Number of chloroplasts and thylakoid membranes decreases under nitrogen deficiency

The total Chl content per leaf area of LN plants was about 50% lower than in HN plants (Table 1). Confocal microscope images showed that in HN plants chloroplasts form dense aggregations along the anticlinal cell walls (Fig. 1a). In LN leaves, the large majority of cells contained only a few single chloroplasts or did not contain chloroplasts at all (Fig. 1b). Some cells contained groups or aggregates of chloroplasts on the anticlinal walls. Furthermore, the fluorescence intensity of individual chloroplasts also appeared to be lower in LN leaves. These data suggest that N deficiency inhibits chloroplast division and leads to decrease in the amount of thylakoid membranes per chloroplast.

N deficiency causes inhibition of photosynthetic reactions in stroma and increases PS I antenna size

The photosynthetic machinery of LN beans was further characterized by quantifying the D1 protein of PS II, the large subunit of Rubisco and FNR in the leaves. N deficiency did not affect D1 content, whereas the amounts of Rubisco and FNR were lower in LN than in HN plants, when measured on Chl basis (Fig. 2). Protein content per leaf area was only 10% lower in LN plants than in HN plants (Table 1), and therefore the low concentrations of FNR and Rubisco indicate specific down-regulation of these enzymes in LN plants. Only small differences in the Chl *a*/*b* and carotenoid/Chl ratio between LN and HN plants were detected, although the total Chl content per leaf area of LN plants was low (Table 1). PS II electron transport activities, measured from isolated thylakoids, were similar in HN and LN plants (Table 1). However, the maximal efficiency of PS II photochemistry $(F_M - F_0)/F_M$, was lower in LN plants than in HN plants (Table 1). PS I activity, measured with MV as electron acceptor, was fairly similar in LN and HN beans (Table 1).

The effect of N starvation on the distribution of excitation energy between PS II and PS I was studied with 77 K emission spectra recorded from crude extracts of HN and LN leaves (Fig. 3). The PS I peak at 733 nm and PS II peak at 685 nm give a F_{733nm}/F_{685nm} ratio of 1.0 in the HN leaves and 1.3 in LN leaves (Fig. 3a). The finding that light-saturated electron transport activities were similar in HN and LN plants (Table 1) suggests that the higher fluorescence emission of PS I of LN plants is due to a larger PS I antenna rather than a larger number of PS I units in LN plants. This hypothesis is supported by the finding that HN beans switched from state 1 to state 2 under illumination with moderate red light (Fig. 3b) but no adjustment of excitation energy distribution occurred in LN plants under the same light treatment (Fig. 3c).

N deficiency slows down electron transfer from Q_A to plastoquinone pool in some PS II centers

The decay of Chl fluorescence yield after a single turnover flash was considerably slower in LN than in HN beans during the first 10 ms after an actinic single turnover flash, while the rest of kinetics did not show any difference (Fig. 4). In general, the kinetics of fluorescence relaxation shows a fast component (about 0.5 ms) related to the re-oxidation of Q_A^- by Q_B, a middle component (about 3 ms) coupled to re-oxidation of Q_A^- by Q_B in centers that have an empty Q_B site, and a slow phase (about 8 s) reflecting recombination between Q_A^- and the S_2 state of the oxygen

Table 1 Pigment and protein contents of leaves and light-saturated activities of partial reactions of photosynthesis in thylakoids isolated from leaves of HN and LN beans, and capacity of PS II photochemistry (F_V/F_M), measured from dark adapted leaves

	Chl ($a + b$), μg cm^{-2}	Chl a/b, μg μg^{-1}	Total protein, mg cm^{-2}	(V + A + Z + N + L)/ Chl a, mmol mol^{-1}	F_V/F_M	O_2 evolution, μmol O_2 (mg Chl)$^{-1}$ h^{-1}	DCIP photo-reduction, μmol DCIP (mg Chl)$^{-1}$ h^{-1}	O_2 consumption ($DCIPH_2 \rightarrow MV$), μmol O_2 (mg Chl)$^{-1}$ h^{-1}
HN	22.6 ± 2.3	3.3 ± 0.3	0.86 ± 0.05	148	0.80 ± 0.016[a]	260 ± 11	129 ± 16	284 ± 6
LN	11.3 ± 1.9	3.1 ± 0.5	0.76 ± 0.07	161	0.71 ± 0.035[a]	288 ± 8	137 ± 11	305 ± 8

V + A + Z + N + L is the sum of violaxanthin, antheraxanthin, zeaxanthin, neoxanthin and lutein. The PPFD of the saturating flash used for the measurement of F_V/F_M was 5,000 μmol m^{-2} s^{-1} and the PPFD used to measure the activities of the partial reactions was approximately 3,000 μmol m^{-2} s^{-1}. Each value represents the mean ± SD of three independent experiments

[a] Each value is an average of eight measurements

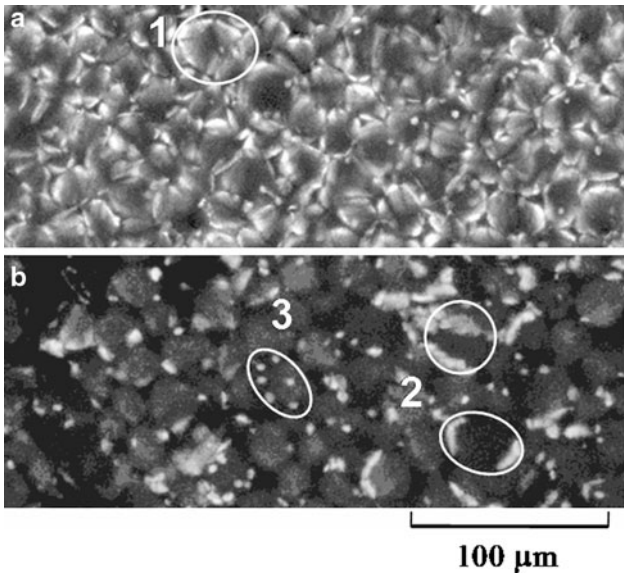

Fig. 1 Confocal microscopy images of Chl autofluorescence from mesophyll cells on the adaxial side of a high nitrogen (HN, **a**) and a low nitrogen (LN, **b**) bean plant. *1* and *2,* cells with chloroplast aggregations; *3*, cell containing several single chloroplasts

evolving complex (OEC) in centers incapable of transferring an electron from Q_A to Q_B. For bean thylakoids, good fits were only obtained if the middle phase was split to two components, referred to as middle phases I and II. The nature of middle phase II remains to be resolved but both lifetime and amplitude of this component were similar in HN and LN samples. The lifetime of the fast component was 2.5-fold and that of the middle component I was 3.0-fold longer in LN than in HN thylakoids, indicating significantly slower electron flow from Q_A to Q_B in LN thylakoids. In LN thylakoids the amplitude of the fast phase was 17% lower and that of the middle phase I was 7% larger than in HN thylakoids. These differences can be explained by assuming that the affinity of PQ to the Q_B-binding site is lower in LN than in HN plants, and therefore the distribution of PS II centers with and without a PQ molecule in the Q_B niche is different in LN and HN plants. The behavior of the slow phase is in agreement with this hypothesis, as the slow phase had two times as high amplitude in LN than in HN plants, indicating that the relative amount of Q_B-non-reducing centers was higher in LN than in HN plants. Alternatively, increase in the slow phases of oxidation of Q_A^- at the expense of the fast phase might suggest that N deficiency lowers the PQ:PS II ratio.

When electron flow between Q_A and Q_B is inhibited, e.g. by 3-(3,4-dichlorophenyl)-1,1-dimethylurea (DCMU), the re-oxidation of Q_A^- proceeds only via charge recombination with donor side components. When the measurements were carried out in the presence of DCMU, the kinetics could be fitted with one hyperbolic decay component with lifetime

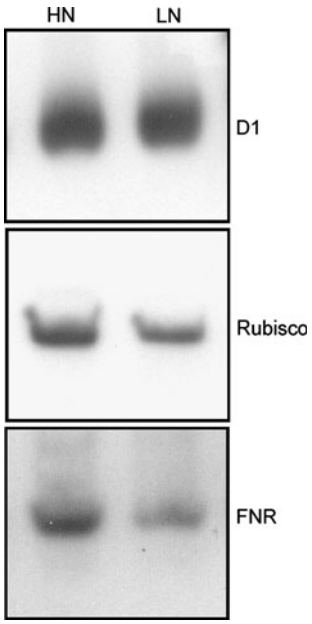

Fig. 2 The D1 protein, Rubisco and FNR contents of *HN* and *LN* samples. One-week-old plantlets were transferred to hydroponic cultures with either the standard growth medium (*HN*) or low nitrogen medium containing only 1% of the standard N concentration (*LN*). Crude extracts and thylakoid samples were isolated after 10 days in the final growth media. Proteins of thylakoid samples (2 μg Chl, used for determination of D1 protein) and crude extracts (0.3 μg Chl for Rubisco and 1.5 μg Chl for FNR) were separated by using NEXT GEL SDS–PAGE and electroblotted to Immobilon-P membranes. The contents of D1 protein, Rubisco and FNR were detected by western blotting using specific antibodies

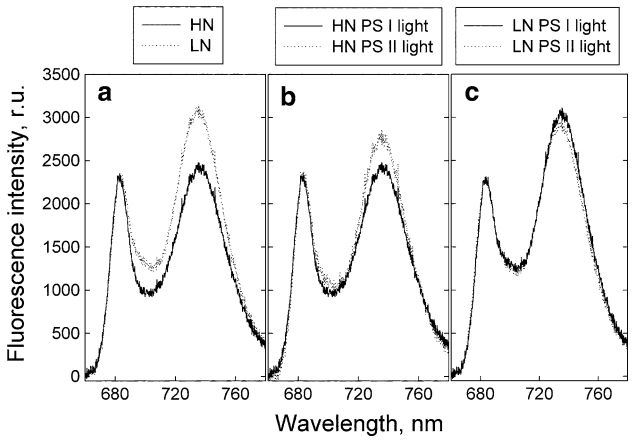

Fig. 3 77 K fluorescence emission spectra of crude extracts from *HN* and *LN* beans. **a** Extracts prepared from dark adapted LN and HN leaves. **b** Extracts prepared from leaves of HN beans. **c** Extracts from leaves of LN beans. Before the preparation of the extracts, the leaves were illuminated with light favoring excitation of PS I (*solid line*, far-red light, 5 min) or PS II (*dotted line*, red light, 20 min, PPFD 100 μmol m^{-2} s^{-1}). The fluorescence spectra were normalized by dividing by the value at 683 nm. All samples were diluted to 10 μg Chl ml^{-1}. A typical result of at least three measurements is shown

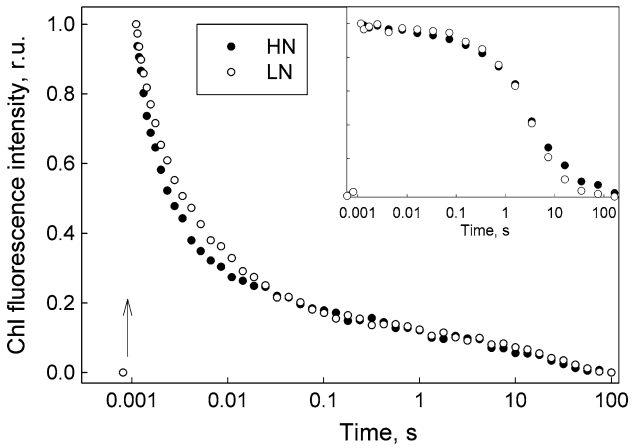

Fig. 4 Dark relaxation Chl fluorescence after a single turnover flash in thylakoid membranes from *HN* and *LN* bean plants. The inset shows measurements performed in the presence of 10 μM DCMU. Each curve is an average of six measurements

of about 5 s in both HN and LN samples (see inset of Fig. 4). This indicates that charge recombination between OEC and Q_A was not altered by N limitation.

Electron transfer between Q_A and Q_B was further studied using TL measurements. In our TL measurements, we first lowered the temperature of the thylakoid sample to −10°C and then fired a short flash to create the state $S_2Q_A^-$ (in the presence of DCMU) or $S_2Q_B^-$ (in the absence of DCMU). Subsequent warming of the sample allowed the charge pair to recombine, producing luminescence. Recombination of the S_2 or the S_3 state of OEC with Q_B^- yields the B band with maximum emission at 30–40°C while in the presence of DCMU the recombination between the S_2 and Q_A^- yields the Q band which peaks at 10–20°C (Vass and Inoue 1992; Tyystjärvi and Vass 2004). The form and peak position of a TL curve show how the rate constant of the respective charge recombination reaction depends on temperature, and TL can therefore be used to calculate the thermodynamic parameters of the recombination reaction.

In thylakoids isolated from HN plants, the B band peaked at 40°C and the Q band at 15°C (Fig. 5). In LN samples, the Q band was found at the same temperature as in the HN sample but the B band was shifted by 7°C toward lower temperature. Model calculations (Table 3; dashed lines in Fig. 5) indicated that the activation free energy of the $S_2Q_B^- \rightarrow S_1Q_B$ recombination was 852 meV for the B band and 787 meV (at 298 K) for the Q band of HN thylakoids, indicating a 65 mV redox potential difference between the Q_A/Q_A^- and Q_B/Q_B^- pairs. The high-temperature side of the B band of the LN thylakoids was wider than found in HN thylakoids, and a good fit could be obtained by assuming that the B band of LN thylakoids consists of a 33% component with the same redox potential of the

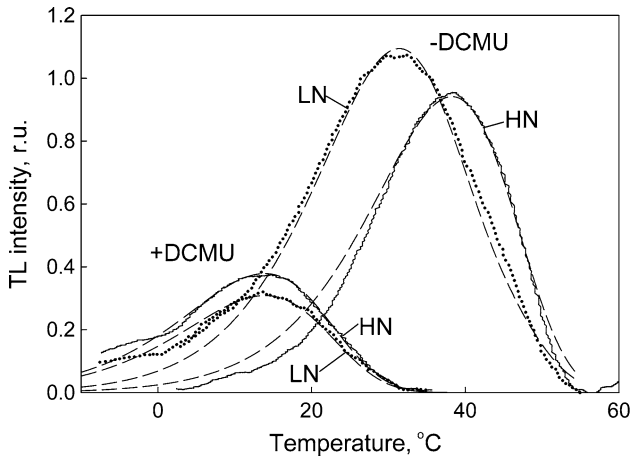

Fig. 5 Thermoluminescence signals measured from thylakoids isolated from *HN* (*solid line*) and *LN* (*dotted line*) bean plants in the absence and presence of 20 μM DCMU, as indicated. Each curve is an average of three measurements. The *dashed lines* show the best fit to the model used to calculate the activation parameters of the recombination reactions

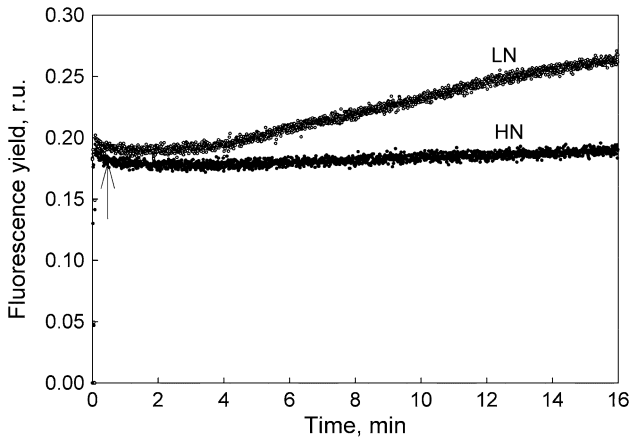

Fig. 6 Changes in Chl fluorescence yield in leaves of *HN* and *LN* beans in the dark under anoxic conditions measured with the PAM 101 fluorometer. The *arrow* indicates the time when anaerobic conditions were established by flushing the sample vial with nitrogen. Before measurements the leaves were dark adapted for 2 h

Q_B/Q_B^- pair as in the HN thylakoids and a 67% component with a 25 mV more reducing Q_B/Q_B^- pair, corresponding with free energy of activation of 827 meV, see Table 3). The best fit was obtained using an activation entropy ($dS^{\updownarrow}$) of 0 for both components of the B band and the value $dS^{\updownarrow} = -0.3$ meV/K for the Q band (Table 3).

N deficiency enhances reduction of the PQ pool by stromal reductants

The PQ pool functions as an electron carrier for both photosynthetic and chlororespiratory electron transport in the chloroplast (Nixon 2000). To measure reduction of PQ by stromal reductants, we illuminated leaves with a weak pulsed measuring beam and measured the minimum fluorescence yield (F_0). In very dim light, the redox state of Q_A is in equilibrium with the redox state of the PQ pool, and reduction of the PQ pool can be detected as an increase in Chl fluorescence yield (Corneille et al. 1998). When dark adapted LN and HN leaves were kept for 1 h under the measuring beam in aerobic conditions, the fluorescence level did not change (data not shown) indicating that the reduction state of the PQ pool remained stable and the pool was mainly oxidized.

The experiment was repeated under pure nitrogen atmosphere where re-oxidation of PQ by the chloroplast terminal oxidase does not function (Corneille et al. 1998; Joët et al. 2002). LN leaves showed rise of the Chl fluorescence yield under nitrogen atmosphere already within the first 15 min of very dim light illumination, while the F_0 level of HN leaf remained fairly stable (Fig. 6). Switching from nitrogen back to air also reversed the F_0 increase (data not shown). As PS II electron transfer activity is similar in LN and HN plants (Table 1), the result suggests that the rate of reduction of the PQ pool by ferredoxin or NAD(P)H is faster in LN than in HN plants.

N deficiency induces cyclic electron flow

In green algae, nitrogen deficiency induces a transition of photosynthetic membranes from state 1 to state 2, which triggers cyclic electron transfer (CET) around PS I (Wykoff et al. 1998; Finazzi et al. 2002). We measured far-red-light-induced redox transitions of P_{700} to see possible changes in electron transfer mode (Fig. 7). If the cyclic mode is dominant, P_{700} oxidation proceeds more slowly than if the linear mode dominates, because CET re-reduces P_{700}^+ by electrons transferred to PQ from Fd or NAD(P)H. In our experiments, dark adapted leaves from HN and LN beans were pre-illuminated by far-red light shortly before measurement in order to induce linear electron transport which operates in light adapted leaves but not in those kept in the dark (Joliot and Joliot 2005). In HN leaves, P_{700} oxidation showed rapid monophasic rise, reaching saturation after about 2 s of illumination (Fig. 7). In LN leaves, rise in P_{700}^+ was much slower and saturation was not reached within 6 s of far-red illumination. This result suggests that in HN leaves, photosynthetic electron flow functions mainly in the linear mode but CET becomes significant in N deficient plants. In agreement with this hypothesis, re-reduction of P_{700}^+ in the dark after far-red illumination was slightly faster in the LN sample (Fig. 7), indicating that the PQ pool was more reduced in LN thylakoids.

P_{700} oxidation showed biphasic kinetics in LN leaves, suggesting the presence of two different populations of chloroplasts. In chloroplasts contributing to the fast phase, PS I centers are involved in linear electron transfer and in chloroplasts showing slow oxidation of P_{700}, PS I centers are mainly involved in CET. Similar biphasic behavior was earlier reported for dark adapted leaves showing elevated CET (Joliot and Joliot 2005). The choice between linear and cyclic mode is done when reduced ferredoxin or NADPH is oxidized, which occurs either in the stroma (linear mode) or at the enzyme(s) mediating oxidation of these compounds by plastoquinone (cyclic mode). Therefore biphasic oxidation of P_{700} rather suggests the presence of two populations of chloroplasts than two populations of PS I centers.

N deficiency causes increase in NPQ

We measured photochemical quenching (q_P) and non-photochemical quenching (NPQ) in leaves of HN and LN beans during illumination with white light, PPFD 300 μmol m^{-2} s^{-1}. After 20 min of illumination, the q_P values of HN and LN leaves were 0.78 and 0.66, respectively, indicating that a smaller fraction of PS II reaction centers were open in LN than in HN plants. Since the proportion of reduced Q_A depends on the balance between excitation of PS II reaction centers and removal of electrons from the electron transport chain, this result testifies for lower capacity to transfer electrons from Q_A to the PQ pool in LN plants, which is in line with the larger proportion of Q_B-non-reducing centers in thylakoids of LN than in HN plants (Table 2). Active CET in chloroplasts of LN plants functions in the same direction, as CET decreases the availability of oxidized PQ.

The light-induced kinetics of NPQ measured from LN and HN beans is shown in Fig. 8. In both types of leaves, NPQ increased to 1.7 during first 1.5 min of illumination. Thereafter, the NPQ value of HN leaves attained a plateau whereas in LN leaves, NPQ continued to increase, reaching a steady state of 2.5 after 5 min of illumination. The increase in NPQ during a few minutes of illumination can be attributed to generation of a transmembrane pH gradient which induces thermal energy dissipation in PS II (Bilger and Björkman 1990). The slope of the initial rise of NPQ was similar in LN and HN leaves, indicating that the light-induced development of thermal dissipation in PS II antenna was not affected by N starvation. The higher final level of NPQ in LN plants reflects stronger acidification of the lumen, probably due to CET operating in N deficient plants (see Fig. 7).

In order to test the effect of the changes in PS II on photosynthesis during N limitation, we measured rapid light response curves with a pulse amplitude modulation fluorometer (Fig. 9). These measurements indicated a lower maximum electron transport rate and larger curvature of the light response but did not reveal differences in the quantum yield (Table 4).

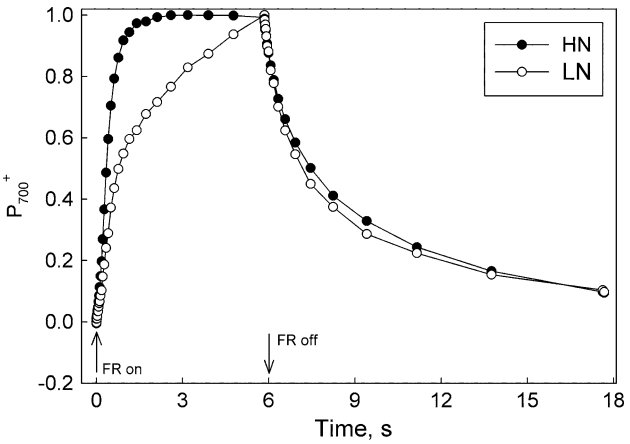

Fig. 7 Kinetics of P_{700} redox transitions measured in leaves of HN and LN beans with a Joliot type spectrometer (JTS-10). Prior to the measurement, the leaves were dark adapted for 2 h, and subsequently exposed to 20 s of far-red pre-illumination and 20 s of darkness. Oxidation of P_{700} was induced with a 6 s pulse of strong far-red light ($700 < \lambda < 800$ nm, 2,500 μmol photons m^{-2} s^{-1}, followed by a 12 s dark relaxation period. Curves were normalized to the maximal amplitude of the signal. A typical result of at least three measurements is shown

Discussion

We found that N deficiency causes four classes of effects in the photosynthetic machinery of bean: properties of PS II are modified, changes on stromal enzymes adjust the ratio of cyclic to linear electron flow, excitation energy distribution between the photosystems is altered, and the number of chloroplasts per leaf cell decreases. These effects are partly independent of each other and partly deeply linked.

N deficiency caused slight lowering of the maximal efficiency of PS II photochemistry in bean plants, in accordance with earlier results obtained with maize and wheat (Lu and Zhang 2000; Lu et al. 2001). LN beans have slower electron transport from Q_A to Q_B, lower redox potential of the Q_B/Q_B^- couple and lower affinity of PQ to the Q_B-binding site than HN beans (Figs. 4, 5; Table 2). In two-thirds of the reaction centers, Q_B^- is less stable than in HN plants, and in one-third, the redox potential of the Q_B/Q_B^- pair remains normal (Table 3). Destabilization of Q_B^- may lower the yield of PS II electron transport under low light intensities where the $S_2Q_B^- \rightarrow S_1Q_B$ recombination reaction has a high quantum yield. These data agree with the finding that the slow phase of the decay of flash-induced Chl *a* fluorescence assigned to the reaction

Table 2 Analysis of the decay of Chl *a* fluorescence yield after a single turnover flash in thylakoids isolated from leaves of HN and LN beans

	Fast phase		Middle phase (I)		Middle phase (II)		Slow phase	
	τ, ms	*A*, %	τ, ms	*A*, %	τ, ms	*A*, %	τ, s	*A*, %
HN	0.45 ± 0.12	70 ± 15	3.1 ± 0.5	16 ± 2	77 ± 11	6 ± 1	8.3 ± 0.8	8.0 ± 0.1
LN	1.02 ± 0.13	53 ± 5	10.4 ± 1.5	23 ± 1	96 ± 29	9 ± 1	9.2 ± 0.9	15 ± 0.6

The numbers represent the lifetime (τ) and amplitude (*A*) ± SE of the estimation

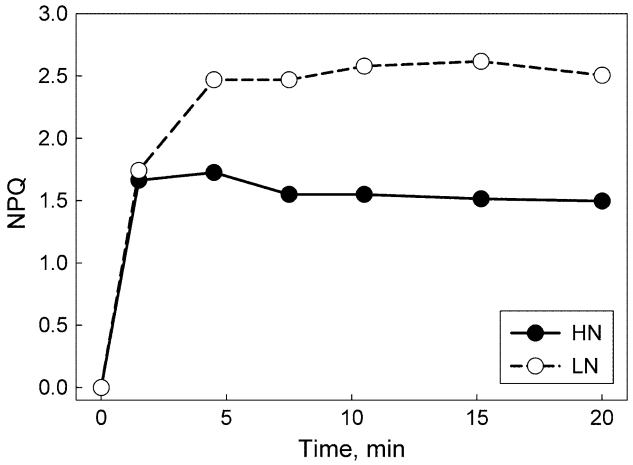

Fig. 8 Light-induced changes of NPQ in leaves of *HN* and *LN* beans measured with PAM 101 fluorometer. The PPFD of actinic light was 300 μmol m^{-2} s^{-1}. Before the measurement, the leaves were dark adapted for 2 h

$S_2Q_B^- \rightarrow S_1Q_B$ showed twice as high amplitude in LN than in HN thylakoids (Table 2). These differences between LN and HN beans show that N deficiency specifically affects the Q_B-binding niche of PS II. The finding that the changes in the Q_B niche do not affect the maximal rate of O_2 evolution or the rate of photochemical reduction of DCPIP (Table 1) is logical because the free energy change of the reaction $Q_A^-Q_B \rightarrow Q_AQ_B^-$ remains strongly negative in LN plants, and therefore the $S_2Q_B^- \rightarrow S_1Q_B$ recombination has a negligible quantum yield under saturating light intensity. The probability of charge recombination actually becomes significant only under very low light, and therefore measurements of the light response of photosynthetic electron transport (Fig. 9; Table 4) did not reveal differences in the quantum yield of PS II electron transport. The data do not allow us to judge whether the changes in the Q_B niche are acclimation or whether they are symptoms of damage.

Slower rate of reoxidation of Q_A^- in LN than in HN thylakoids (Table 2) might additionally suggest that N deficiency lowers the PQ:PS II ratio. However, low amount of PQ would not cause destabilization of Q_B (Table 3) or the lowering of the rate of the fast phase of the reoxidation of Q_A^- (Table 2).

The finding that N deficiency lowers Rubisco content and CO_2 fixation but does not affect activities of photosynthetic electron transport reactions expressed per Chl unit (Fig. 2; Table 1) are in agreement with earlier studies from higher plants (Evans and Terashima 1987; Terashima and Evans, 1988; Seemann et al. 1987). A greatly diminished maximum rate and large curvature of the light response of photosynthetic electron transport of LN beans, compared to HN beans (Fig. 9) confirm that the carbon cycle limits the rate of photosynthesis in LN beans and suggest that the PQ pool of LN plants is reduced already at moderate light intensities. Our data show that in bean, the effect of N limitation goes beyond lowering the Rubisco content, as the amount of FNR, the enzyme responsible for oxidation of ferredoxin and production of NADPH, was also significantly down-regulated upon N starvation. In the absence of alternative electron acceptors, decrease in FNR would lead to increase in reactive oxygen species produced due to reduction of oxygen by PS I (Smirnoff 1993; Asada 2006). This expectation was recently confirmed by showing that transgenic tobacco with reduced level of FNR had visible signs of oxidative stress (Hald et al. 2008).

Prolonged incubation of N deficient beans in the light in the presence of DAB did not reveal accumulation of H_2O_2 (data not shown), suggesting that in LN beans, the decrease in FNR and Rubisco content is compensated by activation of CET. Activation of CET due to low activity of these enzymes is in agreement with data showing that accumulation of stromal reductants during the induction of photosynthesis can activate CET in spinach (Breyton et al. 2006). However, only one of the cyclic electron transfer pathways oxidizes ferredoxin by plastoquinone without involvement of $NADP^+$/NADPH, whereas the other pathway oxidizes NADPH by plastoquinone (Breyton et al. 2006; Rumeau et al. 2007). The low FNR content of LN plants (Fig. 2) suggests that activation of CET in LN beans is mainly activation of the NADPH-independent pathway.

CET contributes to acidification of the lumen (Heber and Walker 1992), which in turn promotes quenching of excitation energy in PS II. Higher NPQ in LN than in HN plants is in agreement with the hypothesis that LN plants have more active CET than HN plants. Moreover, CET does not produce net NADPH for which there is little need when the Calvin–Benson cycle runs slowly. These acclimation responses are summarized in Fig. 10.

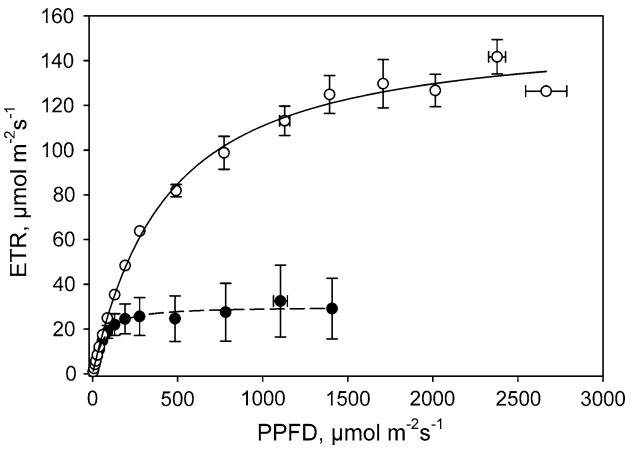

Fig. 9 Light response curve of photosynthetic electron transport of *HN* (*open symbols*) and *LN* beans (*solid symbols*). The light response curves were measured with a pulse amplitude modulation fluorometer, and a leaf was kept for 2 min at each PPFD. Each data point is an average of 5–6 independent measurements from different leaves, and the biaxial *error bars*, drawn if larger than the symbol, show SD. The *lines* show the best fit to the nonrectangular hyperbolic model of the photosynthetic light response curve

Multiple FNR isoforms of plants may have different tasks. Nitrogen supply and leaf development have been shown to affect the distribution of FNR isoforms in wheat leaves (Gummadova et al. 2007), and in Arabidopsis, one isoform is active in CET (Lintala et al. 2007). Changes in the distribution of FNR isoforms, not distinguished by our measurements, may also affect the activity of CET in bean leaves during N starvation.

The third major effect of N deficiency is re-adjustment of the relative antenna cross-sections in favor of PS I, resembling a permanent shift to state 2 (Fig. 3). The finding that light quality failed to cause regular state changes in LN beans suggests that the movable LHCII complexes either do not exist in LN beans or are permanently attached to PS I. In both cases, the excitation energy density in PS II would be lowered both due to decrease in absorption cross-section of PS II and due to NPQ which is enhanced by CET around PS I. The lack of state transitions may be related to the finding that formation of grana stacks is disturbed in chloroplasts of N deficient bean plants (Whatley 1971).

Unlike higher plants, microalgae deprived of macronutrients, such as nitrogen, sulfur or phosphorus, appear to have severe damage of the photosynthetic apparatus, especially PS II, although nutrient limitation triggers redistribution of excitation in favor of PS I and switching of electron flow to CET (Kolber et al. 1988; Wykoff et al. 1998). But how do plants avoid harmful reactions during N deficiency? The results of the present study show that the number of chloroplasts per cell was lower in LN beans than in HN beans, indicating down-regulation of chloroplast multiplication during leaf growth. Moreover, in agreement with a previous ultrastructural study (Whatley 1971), we found that the amount of thylakoid membranes per chloroplast was also reduced. This mechanism apparently adjusts balance between photosynthetic electron transport, Calvin–Benson cycle, and reduced anabolic metabolism. The capacity of N starved plants to tune photosynthetic performance by regulating division of photosynthetic organelles may contribute to protection of the cells from the production of reactive oxygen species.

Increase in F_0 during dark anaerobic incubation (Fig. 6) suggests that the PQ pool was reduced by electron flow from the stromal reductants ferredoxin and NADPH, and the reduction occurred faster in LN than in HN beans. This increase in reduced compounds in the stroma may be caused by electron transport supported by the dim

Table 3 Values of activation entropy ($\Delta S^{\ddagger}$), activation enthalpy ($\Delta H^{\ddagger}$) and free energy of activation ($\Delta G^{\ddagger}$, calculated at 298 K) of PS II recombination reactions calculated from TL curves

Reaction	HN thylakoids				LN thylakoids			
	$\Delta S^{\ddagger}$, meV/K	$\Delta H^{\ddagger}$, meV	$\Delta G^{\ddagger}$, meV	Amplitude, %	$\Delta S^{\ddagger}$, meV/K	$\Delta H^{\ddagger}$, meV	$\Delta G^{\ddagger}$, meV	Amplitude, %
$S_2Q_A^- \rightarrow S_1Q_A$	−0.3	698	787	100	−0.3	698	787	100
$S_2Q_B^- \rightarrow S_1Q_B$, component 1	0	852	852	100	0	852	852	33
$S_2Q_B^- \rightarrow S_1Q_B$, component 2					0	827	852	67

Table 4 Analysis of rapid light response curves from HN and LN beans

	Quantum yield, e^-/photon	Maximum rate, μmol e^- m^{-2} s^{-1}	Curvature
HN beans	0.34 ± 0.04	154 ± 6.7	0.20 ± 0.27
LN beans	0.34 ± 0.05	30.0 ± 1.0	0.59 ± 0.20

PS II electron transport rate was measured with the PAM fluorometer. The values represent the best fit of the light response curves to the nonrectangular hyperbolic model, omitting dark respiration. The values represent the parameters of the best fit and the SE of the estimation using curves averaged from 5–6 independent experiments

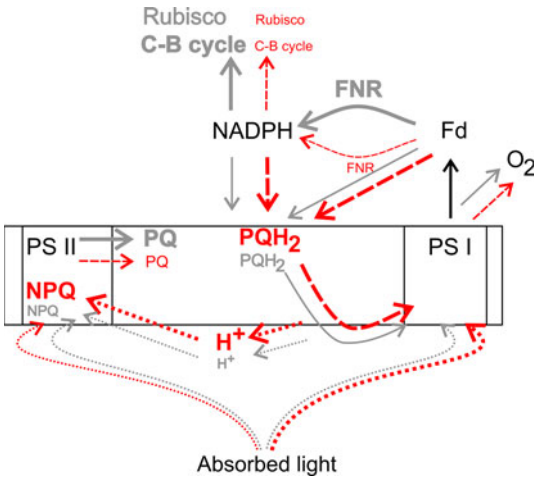

Fig. 10 Summary of acclimation to N deficiency at the chloroplast level. *Grey color* and *continuous line* shows electron transfer reactions in chloroplasts of *HN* plants, *red color* and *dashed lines* show electron transfer reactions in LN plants. *Dotted lines* show other effects than electron transfer. Low Rubisco content and low FNR content switch electron transfer from linear to cyclic mode, which increases the PQH_2/PQ ratio and acidifies the stroma. Higher PQH_2/PQ ratio decreases q_P and acidification of the stroma increases NPQ of LN plants. LN beans are permanently in state 2. The high ratio NAD(P)H/$NAD(P)^+$ promotes non-photochemical reduction of the PQ pool

measuring beam of the fluorometer. In LN plants, the pool of the stromal electron acceptors is rapidly exhausted by the slow electron transport, which leads to activation of CET and reduction of the PQ pool. A high NADPH/$NADP^+$ ratio might also result from the breakdown of starch accumulated upon N starvation; in this case the combination of CET and chlororespiration would explain why the F_V/F_M ratio is only slightly lower in LN than in HN bean plants (Table 1), indicating that the plastoquinone pool does not become reduced in LN plants under aerobic conditions in the dark.

In conclusion, N deficiency induces a complex response, in which the plant down-regulates its photosynthetic capacity. First, the number of chloroplasts and the amount of thylakoids in them decrease. Second, reduction of consumption of photosynthates induces decrease in Rubisco and FNR content, which leads to reduction of CO_2 fixation but not to production of oxygen radicals because CET increases, competing with oxygen for electrons. CET also lowers photochemical quenching and increases non-photochemical quenching in PS II, thus contributing to protection of PS II against photodamage.

Acknowledgments The authors thank Drs. Y. Allahverdiyeva, S. Kangasjärvi, and P. Mulo from Molecular Plant Biology, Department of Biochemistry and Food Chemistry, University of Turku, for ideas and for assistance in experiments. This study was supported by Academy of Finland.

References

Allahverdiyeva Y, Deák S, Szilárd A, Diner BA, Nixon PJ, Vass I (2004) The function of D1–H332 in photosystem II electron transport studied by thermoluminescence and chlorophyll fluorescence in site-directed mutants of Synechocystis 6803. Eur J Biochem 271:3523–3532

Asada K (2006) Production and scavenging of reactive oxygen species in chloroplasts and their function. Plant Physiol 141:391–396

Bilger E, Björkman O (1990) Role of the xanthophyll cycle in photoprotection elucidated by measurements of light-induced absorbance changes, fluorescence and photosynthesis in leaves of *Hedera canariensis*. Photosynth Res 25:173–185

Bondada BR, Syvertsen JP (2003) Leaf chlorophyll, net gas exchange and chloroplast ultrastructure in citrus leaves of different nitrogen status. Tree Physiol 23:553–559

Breyton C, Nandha B, Johnson GN, Joliot P, Finazzi G (2006) Redox modulation of cyclic electron flow around photosystem I in C3 plants. Biochemistry 45:13465–13475

Corneille S, Cournac L, Guedeney G, Havaux M, Peltier G (1998) Reduction of the plastoquinone pool by exogenous NADH and NADPH in higher plant chloroplasts-characterization of a NAD(P)H-plastoquinone oxidoreductase activity. Biochim Biophys Acta 1363:59–69

Curtis VA, Brand JJ, Togasaki RK (1975) Partial reactions of photosynthesis in briefly sonicated *Chlamydomonas*. Plant Physiol 55:183–186

Evans JR, Terashima I (1987) The effects of nitrogen nutrition on electron transport components and photosynthesis in spinach. Aust J Plant Physiol 14:59–68

Finazzi G, Rappaport F, Furia A, Fleischmann M (2002) Involvement of state transition in the switch between linear and cyclic electron flow in *Chlamydomonas reinhardtii*. EMBO Rep 3:280–285

Glasstone S, Laidler KJ, Eyring H (1941) The theory of rate processes. McGraw-Hill, New York

Gummadova JO, Fletcher GJ, Moolna A, Hanke GT, Hase T, Bowsher CG (2007) Expression of multiple forms of ferredoxin $NADP^+$ oxidoreductase in wheat leaves. J Exp Bot 58:3971–3985

Hakala M, Tuominen I, Keränen M, Tyystjärvi T, Tyystjärvi E (2005) Evidence for the role of the oxygen-evolving manganese complex in photoinhibition of photosystem II. Biochim Biophys Acta 1706:68–80

Hald S, Nandha B, Gallois P, Johnson GN (2008) Feedback regulation of photosynthetic electron transport by NAD(P)H redox poise. Biochim Biophys Acta 1777:433–440

Heber U, Walker D (1992) Concerning a dual function of coupled cyclic electron transport in leaves. Plant Physiol 100:1621–1626

Hoagland DR, Arnon DI (1950) The water-culture method for growing plants without soil. Calif Agric Exp Stn Circ 347:1–32

Inskeep W, Bloom PR (1985) Extinction coefficients of chlorophyll a and b in *N*, *N*-dimethylformamide and 80% acetone. Plant Physiol 77:483–485

Jassby AD, Platt T (1976) Mathematical formulation of the relationship between photosynthesis and light for phytoplankton. Limnol Oceanogr 21:540–547

Joët T, Genty B, Josse E-M, Kuntz M, Cournac L, Peltier G (2002) Involvement of a plastid terminal oxidase in plastoquinone oxidation as evidenced by expression of the *Arabidopsis thaliana* enzyme in tobacco. J Biol Chem 277:31623–31630

Joliot P, Joliot A (2005) Quantification of cyclic and linear flows in plants. Proc Natl Acad Sci USA 102:4913–4918

Keren N, Berg A, VanKan PJM, Levanon H, Ohad I (1997) Mechanism of photosystem II photoinactivation and D1 protein degradation at low light: the role of back electron flow. Proc Natl Acad Sci USA 94:1579–1584

Kolber Z, Zehr J, Falkowski P (1988) Effects of growth irradiance and nitrogen limitation on photosynthetic energy conversion in photosystem II. Plant Physiol 88:923–929

Kutik J, Lubomir N, Demmers-Derks HH, Lawlor DW (1995) Chloroplast ultrastructure of sugar beat (*Beta vulgaris* L.) cultivated in normal and elevated CO_2 concentrations with two contrasted nitrogen supply. J Exp Bot 46:1797–1802

Laisk A, Eichelmann H, Oja V, Peterson RB (2005) Control of cyt b(6)/f at low and high light intensity and cyclic electron transport in leaves. Biochim Biophys Acta 1708:79–90

Lawlor DW, Boyle FA, Young AT, Keys AJ, Kendall AC (1987) Nitrate nutrition and temperature effects on wheat: photosynthesis and photorespiration of leaves. J Exp Bot 38:393–408

Lintala M, Allahverdieva Y, Kidron H, Piippo M, Battchikova N, Suorsa M, Rintamäki E, Salminen TA, Aro E-M, Mulo P (2007) Structural and functional characterization of ferredoxin-NADP+-oxidoreductase using knock-out mutants of Arabidopsis. Plant J 49:1041–1052

Lu C, Zhang J (2000) Photosynthetic CO_2 assimilation, chlorophyll fluorescence and photoinhibition as affected by nitrogen deficiency in maize plants. Plant Sci 151:135–143

Lu C, Zhang J, Zhang Q, Li L, Kuang T (2001) Modification of photosystem II photochemistry in nitrogen deficient maize and wheat plants. J Plant Physiol 158:1423–1430

Marschner H (1995) Mineral nutrition of higher plants. Academic Press, San Diego

Nixon PJ (2000) Chlororespiration. Phil Trans R Soc Lond B 355:1541–1547

Pascal AA, Liu ZF, Broess K, van Oort B, van Amerongen H, Wang C, Horton P, Robert B, Chang WR, Ruban A (2005) Molecular basis of photoprotection and control of photosynthetic light harvesting. Nature 436:134–137

Porra RJ, Thompson WA, Kriedemann PE (1989) Determination of accurate extinction coefficients and simultaneous equations for assaying chlorophylls *a* and *b* extracted with four different solvents: verification of the concentration of chlorophyll standards by atomic absorption spectroscopy. Biochim Biophys Acta 975:384–394

Ren D, Yang H, Zhang S (2002) Cell death mediated by MAPK is associated with hydrogen peroxide production in *Arabidopsis*. J Biol Chem 277:559–565

Rumeau D, Peltier G, Cournac L (2007) Chlororespiration and cyclic electron flow around PSI during photosynthesis and plant stress response. Plant Cell Env 30:1041–1051

Sage RF, Pearcy RW (1987) The nitrogen efficiency of C3 and C4 plants. I. Leaf nitrogen effects on the gas exchange characteristics of *Chenopodium album* (L.) and *Amaranthus retroflexus* (L.). Plant Physiol 84:959–963

Schreiber U, Schliwa W, Bilger U (1986) Continuous recording of photochemical and non-photochemical chlorophyll fluorescence quenching with a new type of modulation fluorometer. Photosynth Res 10:51–62

Seemann JR, Sharkey TO, Wang JL, Osmond CB (1987) Environmental effects on photosynthesis, nitrogen-use efficiency, and metabolite pools in leaves of sun and shade plants. Plant Physiol 84:796–802

Smirnoff N (1993) The role of active oxygen in response of plants to water deficit and desiccation. New Phytol 125:27–58

Sugiharto B, Miyata K, Nakamoto H, Sasakawa H, Sugiyama T (1990) Regulation of expression of carbon-assimilating enzymes by nitrogen in maize leaf. Plant Physiol 92:963–969

Terashima I, Evans JR (1988) Effects of light and nitrogen nutrition on the organization of the photosynthetic apparatus in spinach. Plant Cell Physiol 29:143–155

Tyystjärvi E, Karunen J (1990) A microcomputer program and fast analog to digital converter card for the analysis of fluorescence induction transients. Photosynth Res 26:127–132

Tyystjärvi E, Vass I (2004) Light emission as a probe of charge separation and recombination in the photosynthetic apparatus: relation of prompt fluorescence to delayed light emission and thermoluminescence. In: Papageorgiou GC, Govindjee (eds) Chlorophyll *a* fluorescence: a signature of photosynthesis. Advances in photosynthesis and respiration, vol 19. Kluwer Academic, Dordrecht, pp 363–388

Tyystjärvi E, Rantamäki S, Tyystjärvi J (2009) Connectivity of photosystem II is the physical basis of retrapping in photosynthetic thermoluminescence. Biophys J 96:3735–3743

Vass I, Inoue Y (1992) Thermoluminescence in the study of photosystem II. In: Barber J (ed) The photosystems: structure, functions and molecular biology. Elsevier, Amsterdam, pp 259–294

Whatley JM (1971) Ultrastructural changes in chloroplasts of *Phaseolus vulgaris* during development under conditions of nutrient deficiency. New Phytol 70:725–742

Wykoff DD, Davies JP, Melis A, Grossman A (1998) The regulation of photosynthetic electron transport during nutrient deprivation in *Chlamydomonas reinhardtii*. Plant Physiol 117:129–139